THE INFLUENCE OF SOLIDIFICATION PROCESS OF SILICON-RICH FERRO-ALLOYS ON PRODUCT QUALITY.

HALVARD TVEIT [1] and OLA RAANESS [2]

INTRODUCTION.

Ferroalloys are normally added to melts as alloying additives, desoxidants or as metallurgical fuels. The concept of quality is normally connected to factors such as the yield and the composition of the material. Not only a high yield, but even more important is a constant yield in the use of ferroalloys for alloying and desoxydation purposes.

A high and constant yield during dissolution is dependent on constant composition of the material, uniform size, shape and a minimum amounts of fines.

It is commonly accepted that there is a connection between the solidification process and the quality on ferroalloys. However, the topic is not widely described in the literature and a systematic study was therefore carried out in a cooperation between Norwegian Ferroalloy Producers and SINTEF. Mr. H.Tveit has done his Phd /1/ in connection with this research program. The scope of this work was to understand how the solidification process would influence factors as:

- Segregation phenomena.
- Grain growth.
- Understand how solid state phase transformations influences the strength of the material

One of the prime scopes have also been to develop methods which makes it possible to predict capacity and product quality on casting equipment and methods based on computer simulation of the solidification and cooling processes.

1 *Chief Metallurgist Thamshavn Verk ELKEM*

2 *Senior Scientist SINTEF div of Metallurgy N7034 Trondheim Norway*

RESEARCH PROGRAM ON SOLIDIFICATION PROCESSES.

The test program was designed to produce data on ferroalloys solidified over a large range of cooling rates, to produce samples for physical testing and to provide samples for structural studies in the electron microscope. The test program could be split into the following sections:

Laboratory tests

The scope of the laboratory program was to study solidification and grain growth under controlled conditions.

A set of tests with unidirectional solidification of both ferrosilicon and silicomanganese were carried out. In these tests the metal was poured into a mould where side walls and the top are made from isolating material. The mould was equipped with copper bottom which was removed as soon as a thin layer of solid metal is formed. This layer was further cooled with water sprays directed on to the bottom of the metal, while temperatures were monitored continuously at various height above the cooled surface.

Special solidification tests

It was of interest to vary the cooling rate over a large scale to cover all possible cooling rates for industrial processes, and to study the resulting structures and segregation pattern.

The highest cooling rates were produced by pouring hot 75% ferrosilicon metal into cooled heavy copper moulds and cooling rates up to 1170°C/min was obtained as average cooling rates between liquidus temperature and until the metal was solidified.

On the other side, by isolating large volumes of liquid 75% ferrosilicon metal or medium carbon silicomanganese we were able to come down to solidification rates of 0.2°C/min.

Monitoring solidification processes in industrial casting processes.

Solidification rates of industrial processes have been measured during: a. Layer casting of 75%ferrosilicon ,b. Casting ferrosilicon and silicomanganese in sand moulds, c. Casting of ferrosilicon in Elkem wheel.

Product evaluation

During transport and handling of ferroalloys degradation of screened material through both crushing and abrasion will produce sub sized material. The samples produced were therefore tested for their ability to withstand pressure and abrasion strength were measured by the "HANNOVER DRUM" method used by Elkem /2/.

Structure analysis by electron microscopy.

The main structure elements in ferrosilicon with silicon contents above 57% is ζ_α and Si. Major equilibrium structure components in standard silicomanganese would be $(Mn,Fe)_3Si$ and $(Mn,Fe)_5Si_3$.

In order to have a quantitative description of these binding components, a backscatter electron image (BEI) from a JEOL JSM-840 was processed and analyzed in a LINK AN 10000 energy dispersive spectrometer. The image processing system was used to measure area fractions ,grain diameters, crack length within each component and distribution of impurity elements.

The LINK AN 10000 was also used to acquire X-ray maps giving element distribution between the different phases.

Develop and simulate the solidification process on computer.

Full scale solidification tests on liquid metal must be regarded as both time consuming and expensive when new types of casting procedures is going to be implemented into production.

In order to be able to predict metal properties and capacity on solidification processes, a mathematical description of the solidification of ferrosilicon under equilibrium conditions is developed, and used in combination with "the Patran Software system" at ELKEM TECHNOLOGY. The computer has been used to calculate the temperature/time dependence for metal and mould during solidification and cooling of the material.

SOLIDIFICATION PROCESSES.

Normal 75% ferrosilicon with its contaminates of aluminium and calcium is a four component system. Standard silicomanganese could also be considered as a four component system with manganese, silicon iron and carbon as its major components. These four phase diagrams are not available, but in describing the physical properties in view of their crystal structure composition these alloys can be regarded as two component systems.

In 75% ferrosilicon the aluminium and calcium will be found in separate phases as iron-aluminium silicides and as calcium silicides. The volume fractions of these phases are negligible compared to that of the silicon and iron-silicide phase.

In the case of silicomanganese iron has a solubility in the manganese-silicides formed during solidification and they form a major part of the overall structure of siliconmanganese. How the iron content of these components are influencing their physical properties are not known.

Depending on the silicon content in the alloy the carbon will be found as a carbide or as graphite but again in moderate volume fractions.

Solidification of (Mn,Fe)-Si alloys.

In working with standard medium carbon silicomanganese most of the work has been done on alloys with 15-18% Si and 5-15% Fe.
The phase diagrams for Mn-Si and (Mn,Fe)-Si as given by Willners and Ottander /3/ in figure 1 describes a peritectic system where the $(Mn,Fe)_5Si_3$ is precipitated as the primary phase and the $(Mn,Fe)_3Si$ is produced through a peritectic reaction between the remaining melt and the primary phase.

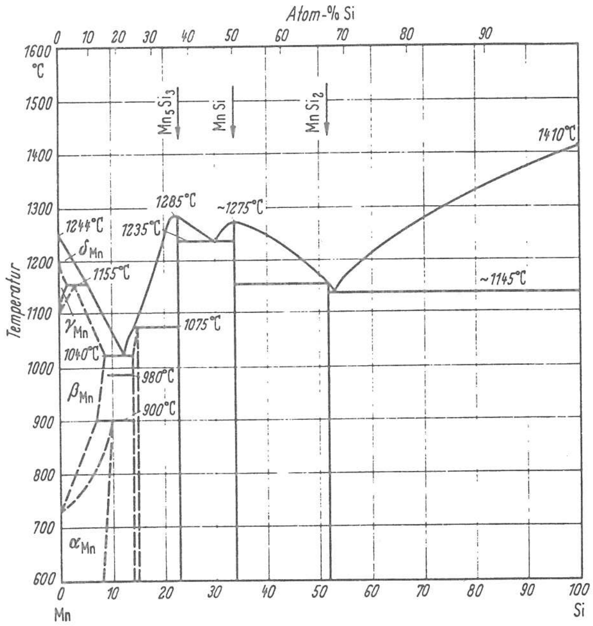

Fig. 1.Phase diagram for Mn-Si. /3/

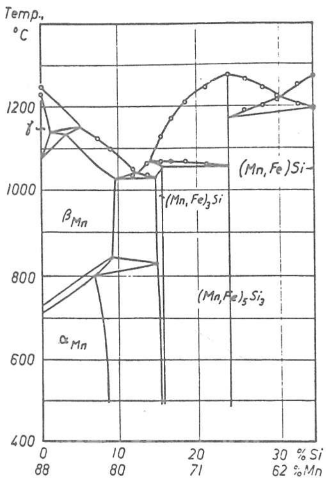

Fig. 2. Phase diagram for (Mn,Fe)-Si. /3/

This peritectic reaction however, implies that diffusion takes place in order to obtain chemical equilibrium. The phase diagrams indicate that these phases are stable down to room temperature.

Solidification of 75% ferrosilicon.

Solidification have been measured at laboratory, in full scale experiments as well as in industrial processes. Temperature measurement have been done with relatively high accuracy in order to be able to detect even small thermal effects during cooling. The experiments have had several objectives:

1. Measurement of cooling rates in the different positions of the castings.

2. Material were sampled close to the thermocouples where the thermal history was known.

3. The temperature-time results from three casting processes were used as cases for numerical modelling of the casting processes.

4. The sampled material were chemically analyses. The result have been used to determine the segregation of the alloys.

The phase diagram for silicon-iron is given in figure 3.

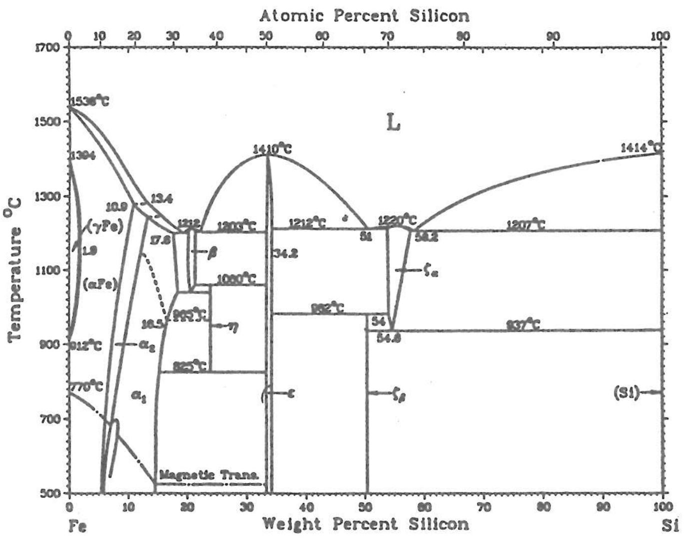

Fig. 3. Phase diagram for Iron-Silicon /4/.

Eutectic solidification in ferrosilicon.

An example of the temperature-time dependencies in four positions for an ingot of 75% ferrosilicon is given i figure 4. This material was cooled in a mould of fines which have a poor heat flux downwards. The dominating heat transport mechanism is radiation from the top surface of the ingot. The size was approximately 2x2 m horizontally and 0,09m in thick.

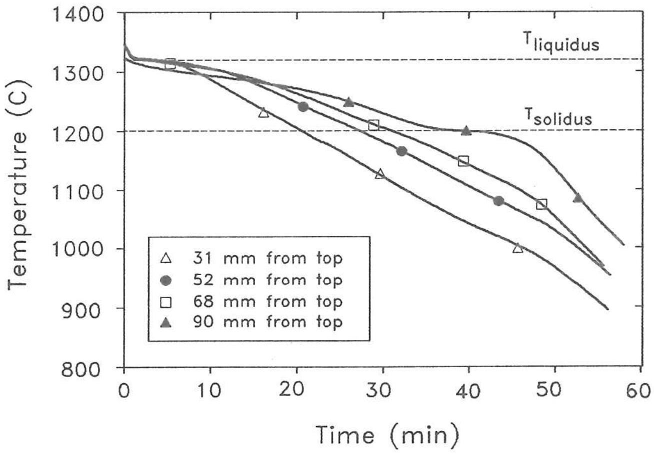

Fig. 4. Temperature-time curves in four positions are given for 75% ferrosilicon solidified in a mould of fines.

Figure 4 shows that the metal in the upper part of the ingot solidifies first. The local solidification time are defined as the time length from the liquid material in one position of an ingot starts to solidify (here 1330°C) until the temperature falls below the eutectic temperature (here 1200°C). The local solidification time varies from approximately 20 min in position 31mm below the top to 40 min in a position 90 mm below the top in figure 4.

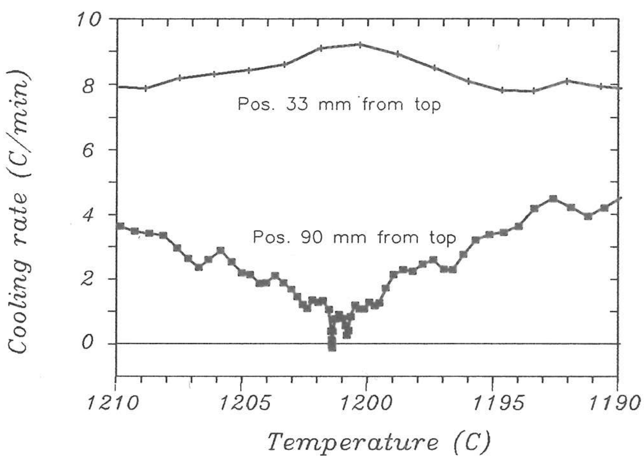

Fig 5. Cooling rate versus temperature through the eutectic temperature regime in 75%ferrosilicon in two different positions.

Figure 4 also shows that the eutectic solidification can be observed on the cooling curves in some positions (here 90 mm from top) while other positions gives little or no indications of the eutectic solidification. In figure 5 the cooling rate through the eutectic temperature in position 31 mm and 90 mm are given. The figure shows no change in the cooling rate for position 31 mm, but a reduction of cooling rate down to 0 °C/min at 1202°C in position 90 mm from top.

This results is typical for what has been observed in most experiments. In positions with high heat fluxes, the heat released through the eutectic solidification can not be seen on the temperature-time curves. In positions with low heat fluxes, however, the eutectic solidification and even the slight heat from solid state transformation can be observed.

Eutectoid reaction in ferrosilicon.

As seen from the phase diagram in figure 3, ferrosilicon with a silicon content exceeding 54.6 wt. % Si the ζ_α is supposed to undergo an eutectoid transformation when the temperature is lower than 937°C:

$$\zeta_\alpha \rightarrow FeSi_2 + Si \qquad (1)$$

In this reaction the high temperature ζ_α -phase (also called a $FeSi_{2.33}$) is transformed through an eutectoid reaction into the low temperature $FeSi_2$ -phase and secondary deposited silicon metal. This reaction have been studied by several authors /5/, /6/, /7/. Normally this reaction have been studied through a prolonged heat treatment. The evidence of reaction (1) have been found by metallographic studies. DeHuff et Al. /6/ have prepared a temperature- time- transformation diagram shown i figure 6. The minimum time for the complete transformation is approximately 6 hours at 700°C.

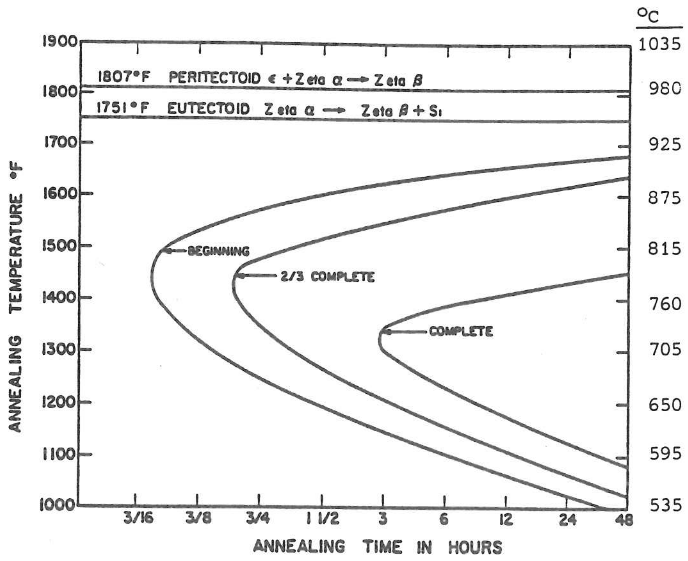

Fig. 6. Temperature-time-transformation diagram for reaction (1). /6/.

Based on single crystal experiments, Boomgard /7/ describes reaction (1) as a two-step reaction:

$$I. \quad (FeSi_{2h}) \rightarrow FeSi_{2r}(Si) \qquad (2)$$

$$II. \quad FeSi_{2r}(Si) \rightarrow FeSi_2 + Si \qquad (3)$$

The first step (eqn. 2) postulates that a supersaturated solid solution of Si in the ζ_α -phase is formed, which is accompanied by a change in volume. This first step is supposed to start at surface irregularities such as cracks and flaws. If there are few such irregularities present the nucleation of the first step will be hampered.

The second step (eqn. 3) takes place in the supersaturated phase where silicon is deposited as a separated phase within the initial ζ_α -grain. Boomgard /7/ describes the total reaction as a polymorphic transformation, followed by a precipitation due to supersaturation.

Only after this precipitation of silicon is it possible to detect the eutectoid reaction by metallographic methods. However, the cooling time for ferroalloys will normally be much shorter than 6 hours and no precipitation pattern is then observed.

The influence on solid state transformations and the strength of silicon containing alloys seems evident.

High-temperature tests on the ferrosilicon material solidified and tested without descending through the eutectoid temperature showed a tensile strength close to that of cast iron. The same test carried out below eutectoid temperature resulted in a complete loss of tensile strength. This difference indicated that major structural changes take place during the cooling through this temperature range.

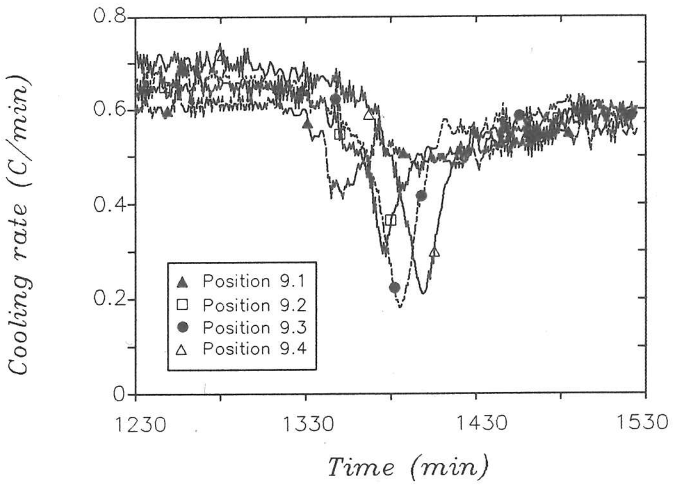

Fig 7. Cooling rate against time through the eutectoid temperature region. The eutectoid transformation does not occur at same time at different positions.

The measurements of cooling rate shows a energy release in the of reduced cooling rates just below the eutectoid temperature. This amount of energy released is stipulated by measuring the temperature at different positions in the alloy. This energy gives a clear deviation from a "normal" cooling rate. As shown in figure 7 and 8 this energy deviation occurs at the same temperature but at different time in the same ingot. The energy is stipulated to 30 kJ/kg ζ_α.

Since no precipitation pattern was observed in samples by metallographic methods, some samples were reheated and annealed at 850°C for 2,4,8,16,32 and 64 min. Samples annealed for 16 min or more shows an increasing amount of equilibrium $FeSi_2$ -phase and deposited silicon. Still after 64 minutes the precipitation step of the eutectoid reaction were not completed.

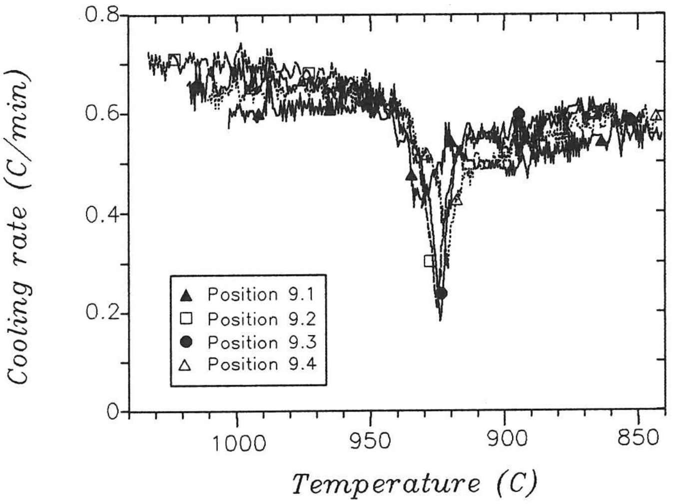

Fig 8. Cooling rate against temperature through the eutectoid temperature region. The eutectoid transformation takes place at the same temperature independent of positions. The numbers gives positions from 40 to 220 mm from top of the ingot.

The solidification and cooling of ferrosilicon as an eutectic and eutectoid system.

By the derivation of the temperature-time curves during solidification and cooling, the cooling rates (°C/min) as a function of the temperature (°C) are determined in figure 9. The cooling process of a 75% ferrosilicon may be grouped into six different process regions.

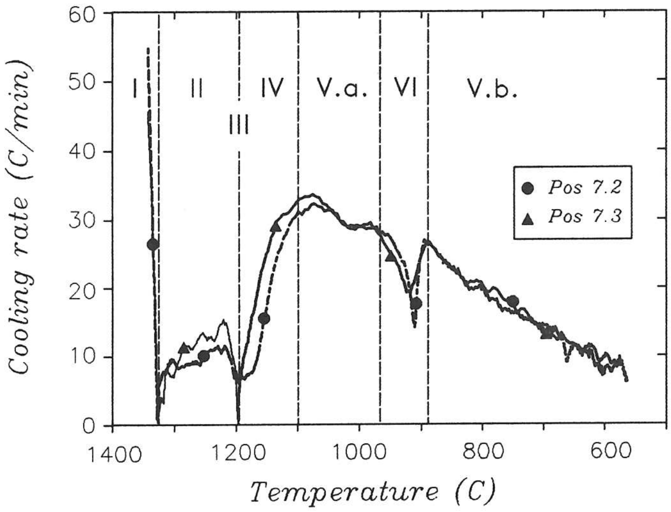

Fig 9. Cooling rate versus temperature for 75% ferrosilicon solidified in an ELKEM casting wheel. Position 7.2 and 7.3 are respectively 51 mm and 68 mm below the surface. Roman numbers I-VI gives temperature intervals for different situations to take place are described in the text.

I. Cooling of liquid. High temperature differences between metal and surroundings and low specific heat capacity gives a high cooling rate.

II. Mushy temperature zone where primary silicon is precipitated. Liberation of large amounts of fusion heat gives a low cooling rate.

III ζ_α is precipitated from the melt during eutectic solidification. The large amount of heat released hamper the cooling.

IV. The material is now solid around the thermocouples, and the cooling rate increases as more and more liquid in rest of the ingot is solidified.

V. Cooling of the solid ingot. The heat capacity is low. The cooling rate decreases as the temperature difference between ingot and surroundings are reduced.

VI. Eutectoid reaction. The energy released through reaction (2) gives a clear reduction in the cooling rate as shown i figure 9.

The solidification and cooling of a ferroalloy in a peritectic solidifying (Mn,Fe)Si alloy.

A similar technique as for 75% ferrosilicon was applied on medium carbon siliconmanganese to study solidification phenomena in a peritectic system and up to 8 distinct temperature regions have been suggested.

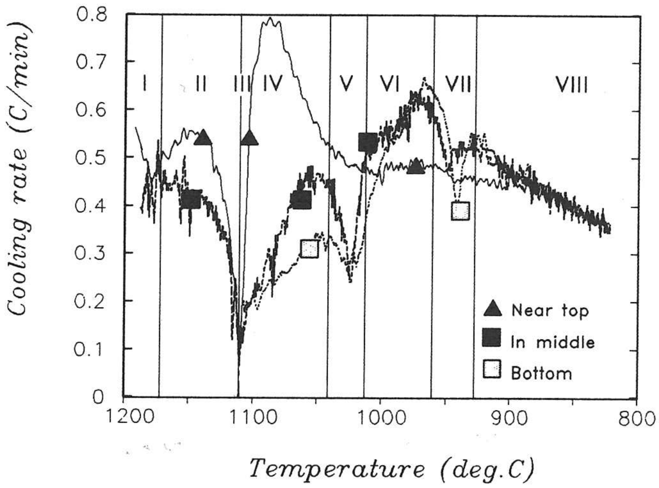

Figure 10 show cooling rate when a thick ingot (500mm) of standard medium C SiMn solidifies. Different reactions takes place in different temperature regions.

I. Liquid metal cools off at a high rate until liquidus temperature is reached.

II. Cooling rate is lowered as heat is released from primary crystallization of $(Mn,Fe)_5Si_3$.

III. A peritectic reaction is suggested to take place at 1110°C.

$4(Fe,Mn)_{(l)} + (Mn,Fe)_5Si_{3(s)} = (Mn,Fe)_3Si_{(s)}$.
The temperature is higher than reported for the Mn-Si system by 35°C.

IV. The increase in cooling rate indicates that the peritectic reaction seizes locally but continues still in other parts of the ingot.

V. The magnitude of drop of cooling rate in the temperature region of 1040-1010°C indicates solid/liquid transformation of material is taking place. The phenomena could be of a "non-equilibrium type of eutectic reaction" resulting in the formation of the $(Mn,Fe)_3Si$ and small amounts of $\beta(Mn,Fe)$. A peritectic reaction could also take place over a temperature interval due to different distribution coefficients between Mn and Fe in liquid and the solid silicides.

VI. The ingot is completely solidified and cooling rate increases.

VII. A drop of cooling rate in the temperature of 960-930°C reveals energy release in the ingot. According to the phase diagrams both the $(Mn,Fe)_5Si_3$ and the $(Mn,Fe)_3Si$ should be stable down to room temperature. The energy release might be caused by differences of thermal properties of major structural components, and a build up of thermal tension followed by release of mechanical energy from friction as the alloy cracks. The loss of strength for medium C silicon manganese is a well known phenomena, but some evidences in our microscopic tests points to instability in the $(Mn,Fe)_5Si_3$ phase.

VIII. Solid material cools down to room temperature.

MODELLING OF SOLIDIFICATION PROCESSES:

To be able to predict the local cooling rate emphasis have been put into modelling of the casting of ferroalloys. The results are used to improve the alloy quality and to improve existing casting processes.

Numerical models of cooling rate

For the casting of 75% ferrosilicon three different casting processes have been both measured and simulated as mentioned before. In the use of a numerical model there are several assumptions that must be taken. The most important assumptions are:

1. A large horizontal dimension compared to alloy thickness gives mainly vertical heat fluxes. This applies both to sand mould casting and the Elkem Casting Wheel and they have therefore been calculated as one-dimensional cases.
This assumption does not hold for the copper mould case and a three- dimensional model was used.

2. Known starting conditions. No attempt has been made to describe filling the mould with molten metal.

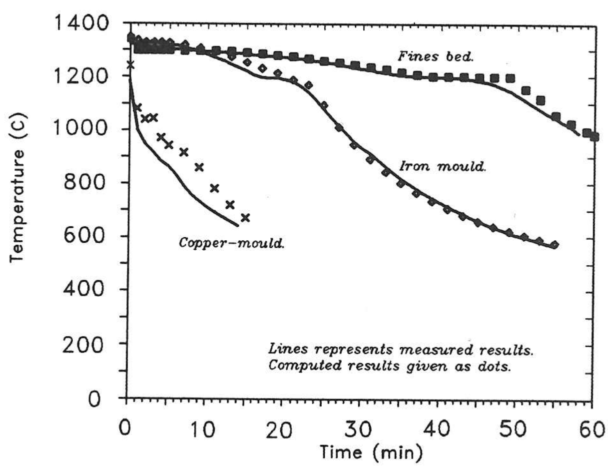

Fig 11 Measured and computed temperature for three casting methods.

3. Equilibrium solidification following the Fe-Si phase diagram.

A "true" entalphy/temperature function including the solidification heats have been developed and used in the numerical model.

Heat transfer to the mould and from the top of the ingot normally controls the cooling rate. Figure 11 shows both measured and calculated temperature-time results for the three different casting methods mentioned.

The casting in the sand-mould gives very low cooling rates because of a low heat flux into the mould. The iron mould gives higher cooling rate as the heat flux to the mould is higher than in the case of the sand mould. Casting into a cobber mould gives a very quick solidification due to the high thermal conductivity of copper. The deviation between the calculated and the computed results for the casting in the cobber mould is mainly due to the fact that filling the mould requires a certain time which is not taken into consideration (assumption 2).

Segregation in 75% ferrosilicon.

Some ferroalloys shows tendencies to segregate. A general reason for segregation are differences in the movement between the solid phase and the liquid phase in the mushy (two-phase) region /8/. Due to a large temperature interval between the liquidus temperature and the solidus temperature the segregation may become severe.

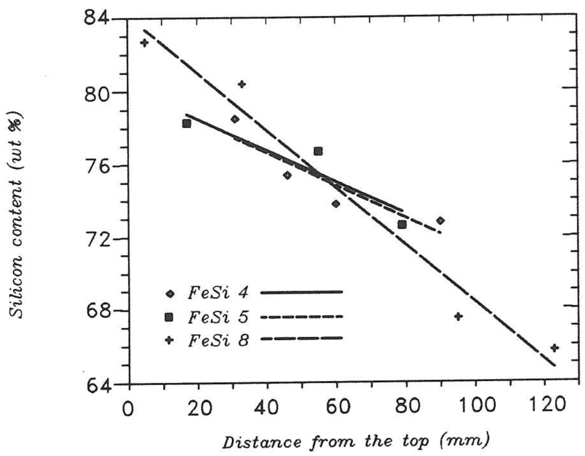

Fig 12. Si-analyses versus distance from the cooling top. FeSi4 and FeSi5 represents moderate cooling rate, in FeSi8 the cooling rate were low.

Segregation in 75% ferrosilicon has been studied both in normal casting and by aggravating the segregating by slow cooling in very thick ingots. The Silicon-content in the thick ingot have been found to vary from 65.7% Si to 83.2% Si.

For 75% ferrosilicon the tendency to segregate is higher with top-cooling than with bottom cooling. This is shown in figure 12 and figure 13. The reason is that the segregation are gravity based. Figure 14A indicates an simplified model for solidification with cooling from the top of the ingot. As initial melt precipitates silicon

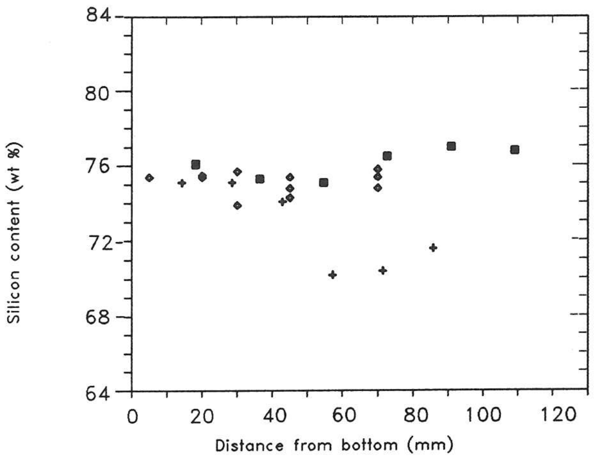

Fig 13. Si-analyses vs distance from the cooling bottom.

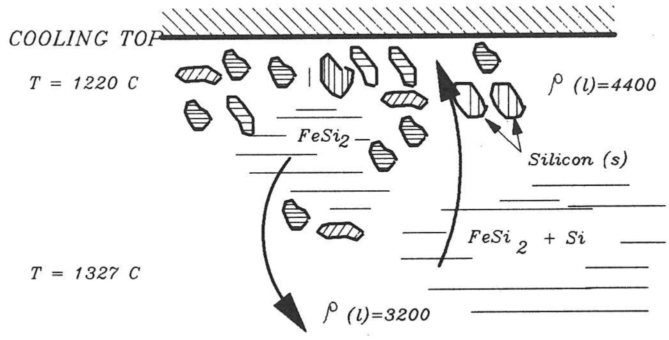

Fig 14A. A segregating model describing bath movement in cooling molten 75% ferrosilicon from the top.

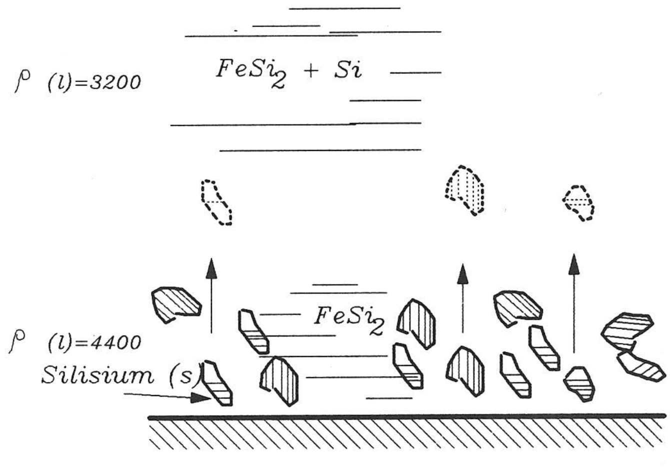

Fig 14B. A segregating model describing bath movement in cooling molten 75% ferrosilicon from the bottom.

crystals the density of the melt will be higher than for the underlying melt, and an unstable occurs with a denser melt above a lighter melt. The difference in density will tend to bring silicon-rich bulk melt up to the mushy zone while iron-rich recycles back into the bulk melt. The overall effect of this backmixing process gives a higher silicon-content at the top of the ingot and the iron-rich melt will concentrate near the bottom of the ingot where it solidifies.

In a similar manner will a bottom cooled situation create a stable situation with a dense liquid phase at the bottom. Flotating silicon crystals tends to be dissolved as indicated in figure 14B.

On the background of the segregation result segregation has been divided into five groups. 1) segregation of the main elements silicon and iron as described above. 2) segregation of elements with little or no solubility in silicon (i.e. Al, Ca and Ti). 3) segregation of elements with major solubility in silicon (i.e. B and P) 4) segregation of Carbon. 5) other gravity segregation (i.e. segregation of inclusions and slags).

I practice casting with cooling both from the top and from the bottom the segregation will be a combination of the results presented in figure 13 and figure 14. It is supposed to give high silicon content at the top of the ingot, average silicon content near the bottom and low silicon content in the middle of the ingot.

STRUCTURE AND STRENGTH:

The strength of an alloy are very much connected with the structure of the alloy. A major part of this study has been to preform metallographic studies on samples which thermal history were known. Different types of strength test have been performed on samples from the same positions in the cast alloy.

Grain size as a function of the cooling rate

The grain diameter has been both measured and calculated. The calculation are based on grain coarsening theory of Kattamis and Flemings /8/. Difference in stability between large grains and smaller grains are the main reason for the grain coarsening mechanisrn. Due to the relative smaller surface energy the large grains are more stable than the smaller grains, and when cooling rates are low this phenomena results in a dissolution of smaller grains and growth of the coarser.

Special methods for measuring an equivalent grain diameter have been developed. Figure 15 shows this grain diameter as a function of the solidification time for SiMn and 75% ferrosilicon. The result for aluminium is published by Flemings /8/.

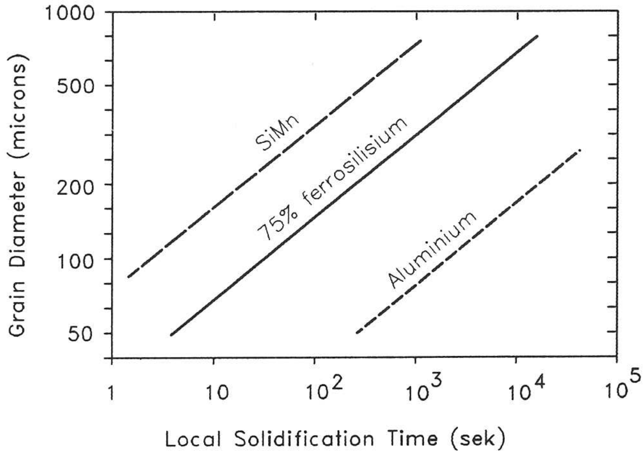

Fig 15. Measured grain diameter as a function of the solidification time for SiMn and 75% ferrosilicon.

Abrasion strength and grain size in 75% ferrosilicon.

In the case of 75%ferrosilicon this material have a typical binding phase and a phase producing tension within the material (ζ_α). As mentioned earlier the local ratio between these two phases may be altered through the segregation phenomena. Distribution of the binding phase are both affected of chemical composition and the grain size (cooling rate).

These connections have been studied by multiregressional analysis based on data obtained on ferrosilicon cast by different methods. Figure 16 represents an "expectation plane" on which properties to expect from different qualities depending upon chemical composition and the casting process.

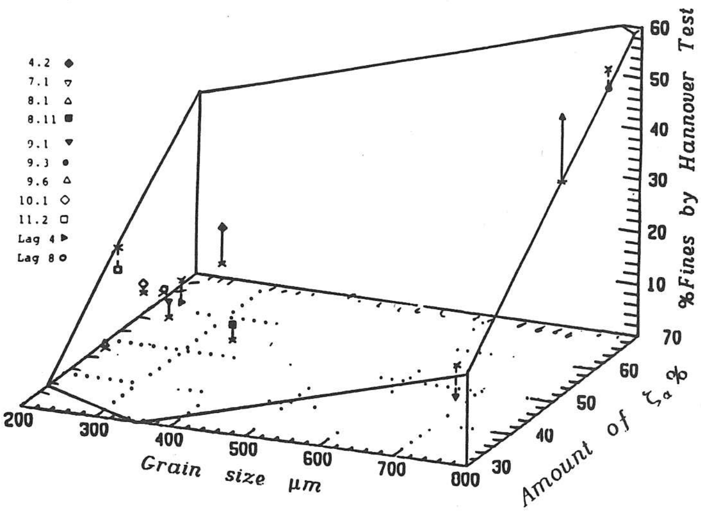

Fig. 16. Abrasion strength against equivalent grain diameter and the amount of ζ_α -phase. Increasing grain size and increasing amount of ζ_α -phase increases the amount of fines (-1 mm).

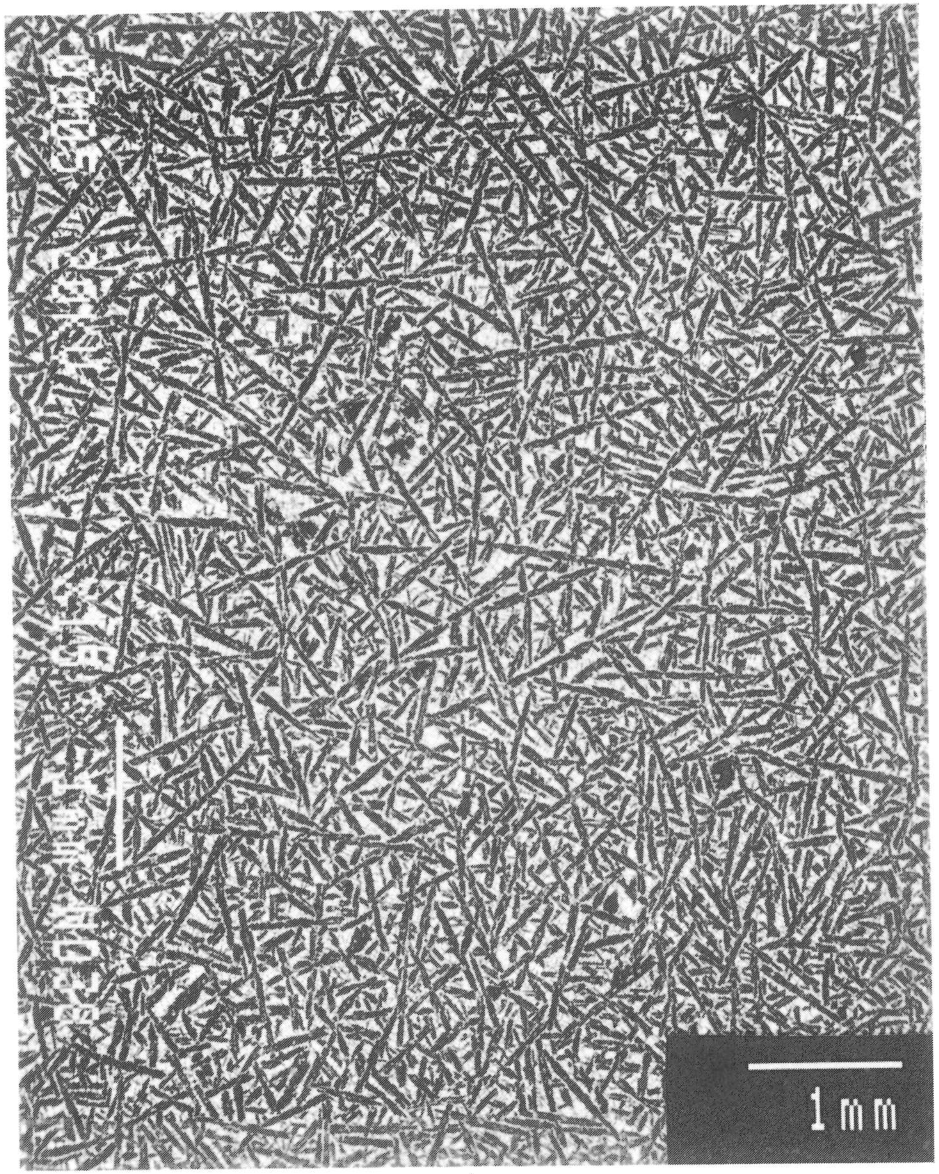

Picture 1 show as an example 75% ferrosilicon s5 olidified with a rate of 1170 °C/min and an equivalent grain diameter of 59µm.

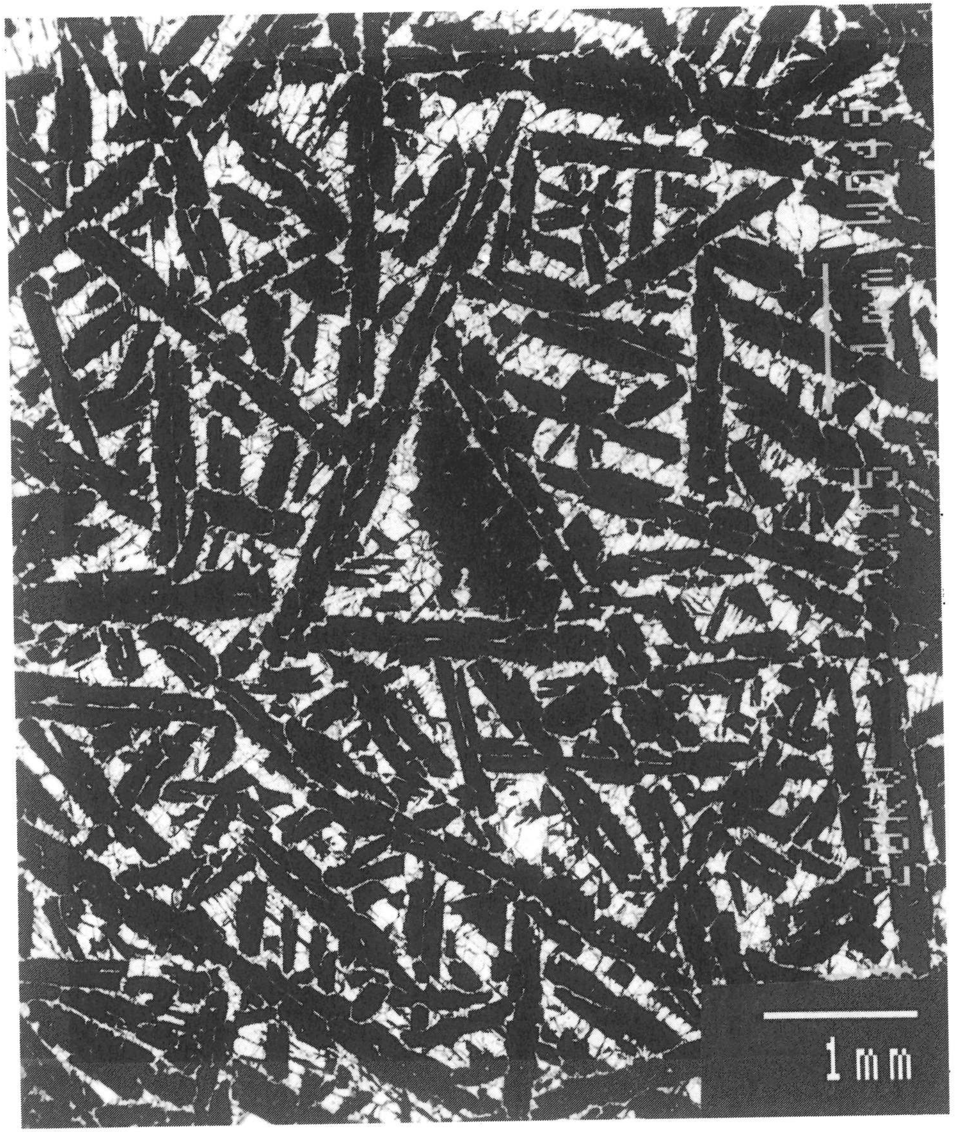

Picture 2 is the same structure solidified with a rate of 20.3 °C/min and a similar grain diameter of 260µm.

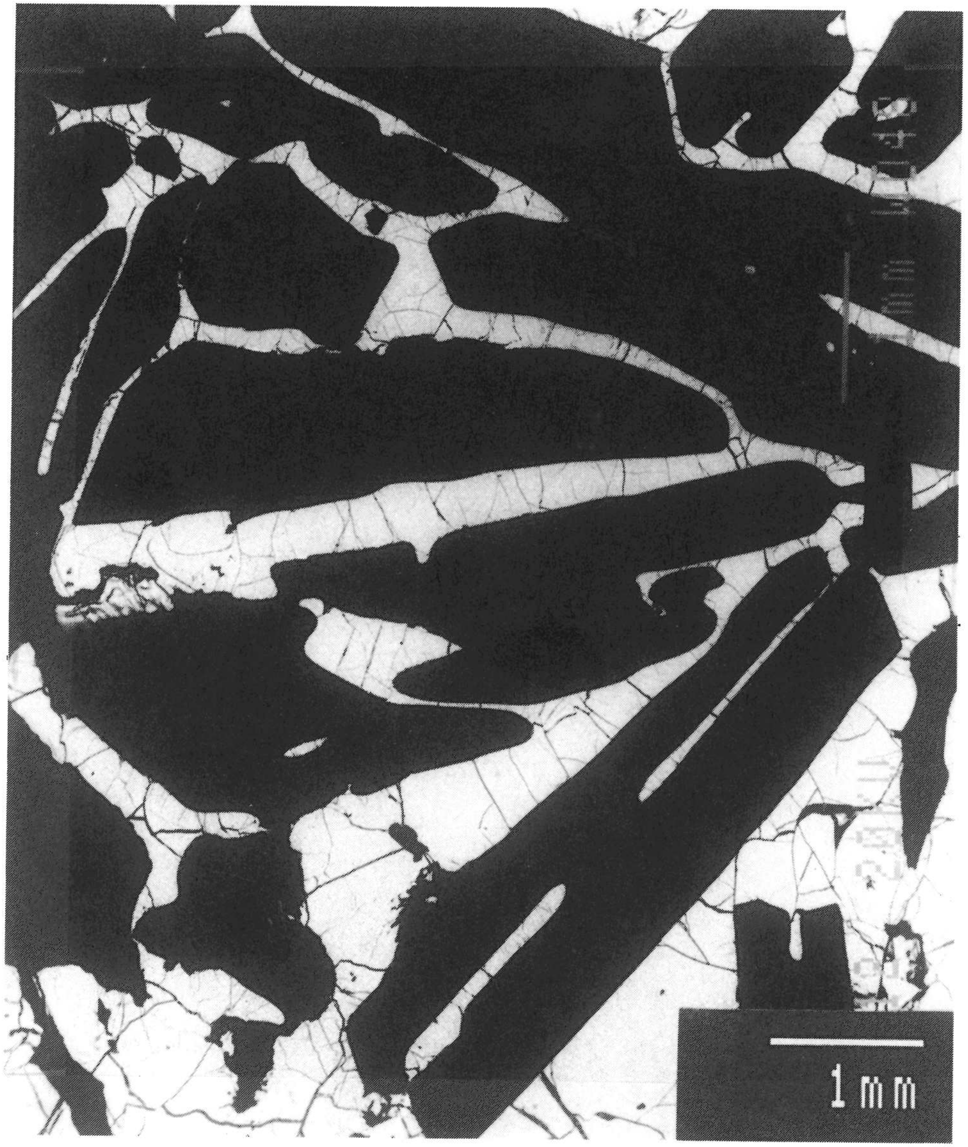

Picture 4 shows the lowest solidification rate with 0.21°C/min and a grain diameter of 784 μm

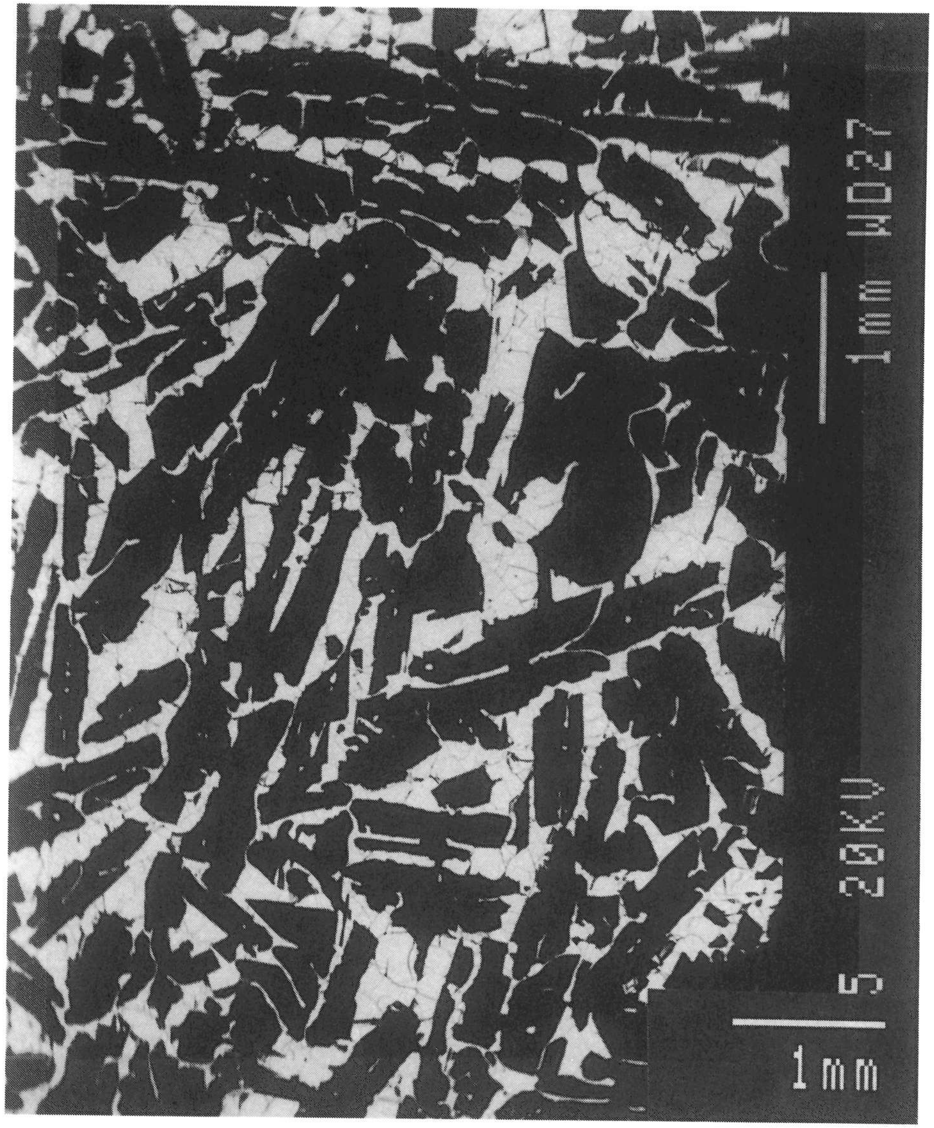

Picture 3 gives the structure at a rate of 7.2°C/min and similar grain diameter of 422μm

Calculation and measurement of grain size in castings.

By combining numerically computed solidification times through the ingot and the relationship between equivalent grain diameter and the solidification time, product properties can be predicted for new processes.

Figure 17 shows both measured and computed equivalent grain diameters through an ingot obtained in three different casting processes.

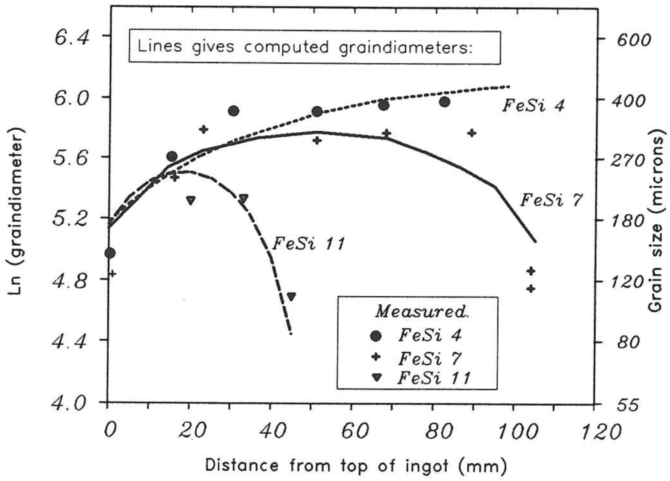

Fig 17. Measured and computed grain diameter through a ingot cast in three different casting methods being (FeSi4) sand mould, (FeSi7) Elkem Wheel, (FeSi11) Copper mould.

Acknowledgements:

We wish to thank the Norwegian Concil of Technology (NTNF) for financial support. We also appriciate financial and technical support from the Norwegian Ferro-Alloy Industry. Major part of the plant test have been carrieed out at Thamshavn Verk and the Tinfos plant at Øye. The numerical calculations have been performed at Elkem Technology and the strength test at the Elkem Research Centre. Valuable assistance are given by P.O. Johnsen, S. Grådahl and N. Andersen at SINTEF.

REFERENCES:

/1/ TVEIT, H.: Solidification of 75% ferrosilicon. *Ph.d thesis.* NTH ISBN82-7119-073-3 Trondheim 1988 (In Norwegian).

/2/ ELKEM Research Centre Vågdsbygd Norway.

/3/ WILNERS/OTTANDER: Manganlegeringar, Jernkontoret 1954 (Sweden)

/4/ KUBASCHEWSKI, O.: Ref: THADDEUS, B.M. m.fl.: Binary Alloy Phase Diagram. *Am. Soc. for Metals*, Oct.1986 p. 1108.

/5/ HOLDHUS, H. The transformation of the ζ-phase in iron-silicon alloys. *J. Iron and Steel Inst.* p.1024-1032 Dec 1962.

/6/ DeHUFF, J.A.: The Structure of Ferrosilicon. *Electric Furnace Proceedings* p.167-174 1969

/7/ BOOMGARD, J. Van den.: Stability of the high-temperature phase $FeSi_2$. *J. Iron and Steel Inst.* p 276-279. April 1972.

/8/ FLEMINGS,M.C.: Solidification Processing *McGraw-Hill Book Company* New York 1974.

/9/ KATTAMIS, T.Z. m.fl.: Influence of Coarsening on Dendrite Arm Spacing of Aluminium-Copper Alloys. *Trans. Met. Soc. AIME* **249** Oct 1967 s 1504-1511.